AMERICAN SOCIETY FOR MICROBIOLOGY | Journal of Virology®

VIRUS-CELL INTERACTIONS

RNA Helicase DDX17 Inhibits Hepatitis B Virus Replication by Blocking Viral Pregenomic RNA Encapsidation

Richeng Mao,[a,b] Minhui Dong,[b,c,d] Zhongliang Shen,[b] Hu Zhang,[a,c,d] Yuanjie Liu,[a,c] Dawei Cai,[a] Bidisha Mitra,[a,c,d] Jiming Zhang,[b] Haitao Guo[a,c,d]

[a]Department of Microbiology and Immunology, Indiana University School of Medicine Indianapolis, Indianapolis, Indiana, USA
[b]Department of Infectious Diseases, Huashan Hospital, Fudan University, Shanghai, China
[c]Department of Microbiology and Molecular Genetics, University of Pittsburgh, Pittsburgh, Pennsylvania, USA
[d]Cancer Virology Program, UPMC Hillman Cancer Center, University of Pittsburgh, Pittsburgh, Pennsylvania, USA

ABSTRACT DDX17 is a member of the DEAD-box helicase family proteins involved in cellular RNA folding, splicing, and translation. It has been reported that DDX17 serves as a cofactor of host zinc finger antiviral protein (ZAP)-mediated retroviral RNA degradation and exerts direct antiviral function against Raft Valley fever virus through binding to specific stem-loop structures of viral RNA. Intriguingly, we have previously shown that ZAP inhibits hepatitis B virus (HBV) replication through promoting viral RNA decay, and the ZAP-responsive element (ZRE) of HBV pregenomic RNA (pgRNA) contains a stem-loop structure, specifically epsilon, which serves as the packaging signal for pgRNA encapsidation. In this study, we demonstrated that the endogenous DDX17 is constitutively expressed in human hepatocyte-derived cells but dispensable for ZAP-mediated HBV RNA degradation. However, DDX17 was found to inhibit HBV replication primarily by reducing the level of cytoplasmic encapsidated pgRNA in a helicase-dependent manner. Immunofluorescence assay revealed that DDX17 could gain access to cytoplasm from nucleus in the presence of HBV RNA. In addition, RNA immunoprecipitation and electrophoretic mobility shift assays demonstrated that the enzymatically active DDX17 competes with HBV polymerase to bind to pgRNA at the 5′ epsilon motif. In summary, our study suggests that DDX17 serves as an intrinsic host restriction factor against HBV through interfering with pgRNA encapsidation.

IMPORTANCE Hepatitis B virus (HBV) chronic infection, a long-studied but yet incurable disease, remains a major public health concern worldwide. Given that HBV replication cycle highly depends on host factors, deepening our understanding of the host-virus interaction is thus of great significance in the journey of finding a cure. In eukaryotic cells, RNA helicases of the DEAD box family are highly conserved enzymes involved in diverse processes of cellular RNA metabolism. Emerging data have shown that DDX17, a typical member of the DEAD box family, functions as an antiviral factor through interacting with viral RNA. In this study, we, for the first time, demonstrate that DDX17 inhibits HBV through blocking the formation of viral replication complex, which not only broadens the antiviral spectrum of DDX17 but also provides new insight into the molecular mechanism of DDX17-mediated virus-host interaction.

KEYWORDS DDX17, encapsidation, hepatitis B virus, pgRNA, viral replication

More than 257 million people are chronically infected with hepatitis B virus (HBV) worldwide, harboring increased risk of developing liver fibrosis, cirrhosis, and primary hepatocellular carcinoma (HCC), which are responsible for over 0.8 million deaths per year. Therefore, there is an urgent unmet need for HBV basic research and antiviral development (1).

Citation Mao R, Dong M, Shen Z, Zhang H, Liu Y, Cai D, Mitra B, Zhang J, Guo H. 2021. RNA helicase DDX17 inhibits hepatitis B virus replication by blocking viral pregenomic RNA encapsidation. J Virol 95:e00444-21. https://doi.org/10.1128/JVI.00444-21.

Editor J.-H. James Ou, University of Southern California

Address correspondence to Haitao Guo, guoh4@upmc.edu.

Received 12 March 2021
Accepted 7 July 2021
Accepted manuscript posted online 21 July 2021
Published 9 September 2021

HBV is a hepatotropic DNA virus belonging to the *Hepadnaviridae* family. The virion particle consists of an outer envelope and an inner icosahedral capsid housing the 3.2-kb partially double-stranded relaxed circular DNA (rcDNA) genome (2, 3). Upon entry into hepatocytes via sodium taurocholate cotransporting polypeptide (NTCP) receptors (4), the viral rcDNA is imported into the nucleus and converted into an episomal covalently closed circular DNA (cccDNA), which serves as the template for generating all viral transcripts, including the 3.5-kb precore mRNA and pregenomic RNA (pgRNA), 2.4- and 2.1-kb surface (envelope) mRNA, and 0.7-kb X mRNA (5, 6). In the cytoplasm, pgRNA is translated into viral core proteins (HBc) and polymerase (pol), the latter *in situ* binds to a stem-loop structure at the 5′ terminus of pgRNA, termed epsilon (ε), triggering encapsidation of the pol/pgRNA complex (7, 8). After nucleocapsid assembly, the encapsidated pgRNA is reverse transcribed into rcDNA by the pol, and then the mature capsid can either be enveloped and secreted or redirected into the nucleus to replenish the cccDNA pool (9, 10).

With a small genome encoding all the constitutive viral components but only one enzyme, HBV replication cycle is, thus, highly dependent on host functions, which positively or negatively regulate viral replication at various steps (6). We have previously demonstrated that the cellular zinc finger antiviral protein (ZAP) is an intrinsic suppressor of HBV replication through promoting viral RNA decay (11). ZAP was initially discovered as a host antiretroviral factor that binds to retroviral RNA and recruits cellular RNA processing exosome complex for RNA degradation (12–14). In addition, cellular DDX17 helicase (also known as p72) has been identified as a ZAP-interacting cofactor that optimizes its antiviral activity against retroviral RNA (15). DDX17 is a member of the Asp-Glu-Ala-Asp (DEAD)-box helicase family, which is involved in various aspects of RNA metabolism, including mRNA transcription, translation, and RNA decay (16). Aside from interacting with ZAP, DDX17 has been found to restrict Rift Valley fever virus (RVFV) via binding to the host and viral stem-loop structures of RNA molecules for dual functions, which regulates endogenous microRNA biogenesis in the nucleus and conducts surveillance against structured non-self RNA elements in the cytoplasm (17). Intriguingly, HBV pgRNA also possesses a stem-loop structure, ε, which is the major structural element in the mapped ZAP-responsive element (ZRE) of the HBV RNA genome (11), raising a research question of whether DDX17 has any antiviral activity against HBV in a ZAP-dependent manner.

In the present study, we identified DDX17 as a host-intrinsic, non-interferon-inducible factor that restricts HBV DNA replication. The DDX17-mediated antiviral effect is an event independent of ZAP-mediated HBV RNA decay but primarily targets the pgRNA encapsidation step. Mechanistic studies revealed that DDX17 binds to the stem-loop structure ε of pgRNA and blocks pgRNA encapsidation in a helicase-dependent manner. The results presented here shed new light on virus-host interaction during HBV infection and may aid the development of novel host-targeting agents for HBV therapeutics.

RESULTS

Expression of DDX17 in cell cultures. To assess the endogenous expression of DDX17 in cell cultures, we detected and compared its endogenous levels among different cell lines by Western blotting. In hepatoma cell line HepG2, Huh7, and HepG2-derived tet-inducible HBV stable cell line HepDES19 and HEK293T cells, the two isoforms of DDX17, including p82 with a molecular weight of 82 kDa and p72 of 72 kDa, are constitutively expressed at similar levels (Fig. 1A). It is known that, by using an upstream non-AUG translation initiation codon, p72 mRNA is alternatively translated into p82, which possesses the biological properties almost identical to those of p72 (18). However, the plasmid FLAG-DDX17, which harbors the open reading frame (ORF) of p72 fused with an N-terminal FLAG tag sequence under the control of a cytomegalovirus immediate-early (CMV-IE) promoter, exclusively expresses the FLAG-tagged p72. Interestingly, the overexpression of p72 significantly reduced the expression of endogenous p82 in HepG2 cells (Fig. 1B). Such autoregulation of DDX17 and its paralog DDX5 has been previously

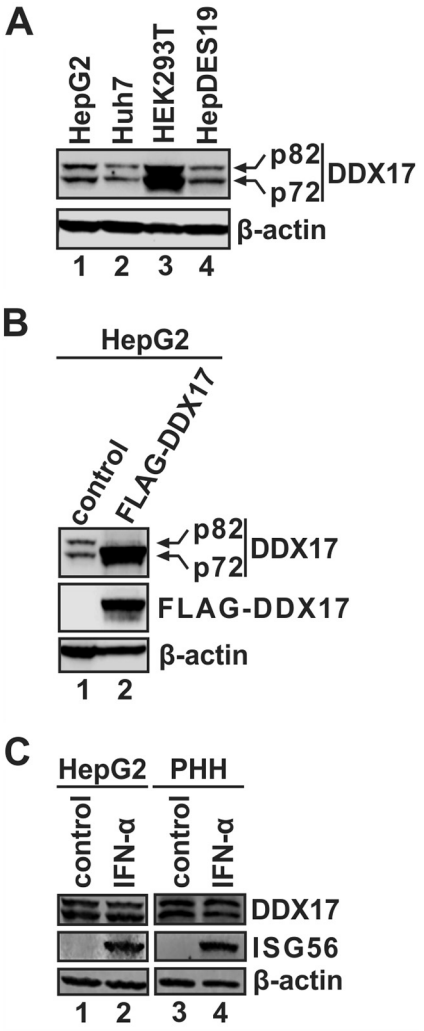

FIG 1 Assessment of DDX17 expression in cell cultures. (A) HepG2, Huh7, HEK293T, and uninduced HepDES19 cells were harvested 36 h after reaching confluence. Endogenous DDX17 levels were detected by Western blotting. β-Actin served as a loading control. (B) HepG2 cells were transfected with control plasmid or FLAG-DDX17 for 4 days. The endogenous DDX17 and FLAG-tagged DDX17 were detected by Western blotting using antibodies against DDX17 and FLAG epitope, respectively. (C) HepG2 and PHH cells were left untreated or were treated with IFN-α (1,000 IU/ml) for 48 h. The expression levels of DDX17 and ISG56 were determined by Western blotting.

reported, and the underlying mechanism is related to their regulatory functions in mRNA splicing and nonsense-mediated mRNA decay (NMD) (19, 20). Furthermore, both p72 and p82 are expressed in primary human hepatocytes (PHH) at similar levels in HepG2 cells and cannot be further upregulated by alpha interferon (IFN-α), indicating that DDX17 is not an interferon-stimulated gene (ISG) (Fig. 1C).

DDX17 is dispensable for ZAP-mediated HBV RNA decay. ZAP is a cellular zinc finger antiviral protein that promotes the degradation of viral RNA, including retroviruses, alphaviruses, filoviruses, and HBV (11, 21). It has been previously reported that DDX17 serves as a cofactor to optimize ZAP-mediated retroviral RNA degradation through facilitating the formation of ZAP-exosome RNA degradation apparatus and/or restructuring the RNA substrate (15). Therefore, it is of interest to assess the potential role of DDX17 in ZAP-mediated HBV RNA degradation. To this end, we assessed the antiviral activity of ZAP-S (the short isoform of ZAP) in HBV-transfected HepG2-NTCP cells with and without stable knockdown of DDX17. As shown in Fig. 2, depleting DDX17 did not markedly alter the steady-state levels of HBV RNA in the absence of

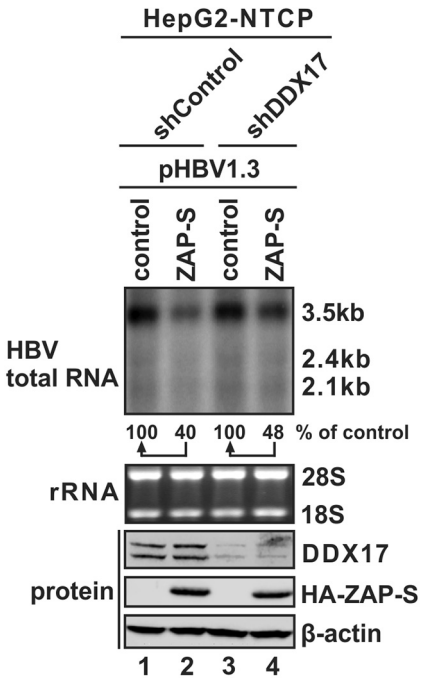

FIG 2 DDX17 is dispensable for ZAP-mediated HBV RNA degradation. Control vector or HA-ZAP-S was cotransfected with pHBV1.3 into HepG2-NTCP-shControl and HepG2-NTCP-shDDX17 cells. Five day after transfection, cells were harvested for HBV total RNA analysis by Northern blotting. The 3.5-kb precore mRNA and pgRNA and 2.4/2.1-kb surface mRNA are indicated. rRNA (28S and 18S) served as an RNA loading control. The protein expression levels of DDX17 and HA-ZAP-S were detected by Western blotting. β-Actin served as a protein loading control.

ZAP-S overexpression or the extent of HBV RNA reduction caused by ZAP-S overexpression, which indicated that DDX17 may not be involved, or at least not absolutely required, in ZAP-mediated HBV RNA degradation.

DDX17 inhibits HBV replication through blocking pgRNA encapsidation. While DDX17 does not seem to significantly regulate HBV RNA stability, in order to assess whether DDX17 possesses any antiviral effect on HBV replication at other steps, we cotransfected pHBV1.3 and FLAG-DDX17 into HepG2 cells and analyzed the major viral replication intermediates and products. As shown in Fig. 3, the ectopically expressed DDX17 (p72) dose-dependently inhibited HBV DNA replication primarily by reducing the levels of encapsidated pgRNA without downregulating the levels of HBV total RNA and precore/core protein expression. Furthermore, knockdown of endogenous DDX17 significantly upregulated the levels of encapsidated HBV pgRNA and core DNA in HepDES19 cells without affecting the steady-state levels of HBV total RNA or core protein (Fig. 4).

Similar phenotypes were observed in HBV-infected HepG2-NTCP cells. After 9 days of HBV infection, the HepG2-NTCP-shDDX17 cells supported higher levels of encapsidated pgRNA and core DNA than control knockdown cells (Fig. 5A), consistent with the findings from the transient-transfection system and HBV-inducible stable cell line (Fig. 3 and 4). Interestingly, the upregulation of HBV core DNA in HepG2-NTCP-shDDX17 cells was mainly revealed by single-stranded DNA (ssDNA) and partially double-stranded DNA, but not the relaxed circular DNA (rcDNA) (Fig. 5A, bottom). A plausible explanation for this observation is that the majority of rcDNA in HBV-infected HepG2-NTCP cells represents the inoculated rcDNA from HBV virions, while the ssDNA and partially double-stranded DNA are better indicators for *de novo* HBV replication. Furthermore, the level of HBV total RNA was found to be higher in HepG2-NTCP-shDDX17 cells than control knockdown cells upon HBV infection (Fig. 5A, top), which was consistent with the higher level of cccDNA transcription templates produced via intracellular cccDNA amplification (Fig. 5B). Nonetheless, another

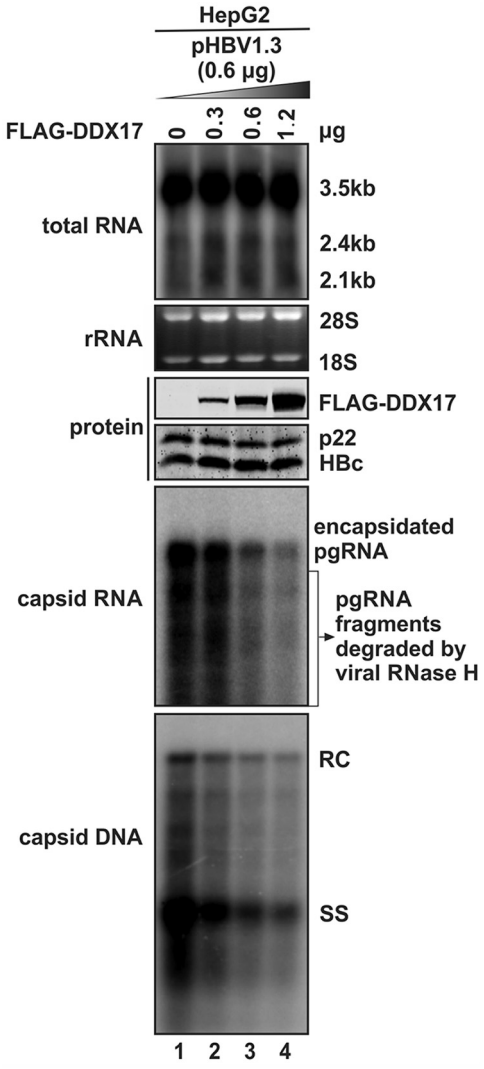

FIG 3 Overexpression of DDX17 inhibits HBV replication primarily by blocking pgRNA encapsidation in a dose-dependent manner. HepG2 cells were cotransfected with 0.6 μg of pHBV1.3 and the indicated amounts of FLAG-DDX17. Control vector was supplemented to normalize the total amount of transfected plasmids to 1.8 μg/transfection. Cells were harvested at day 5 posttransfection, and HBV total RNA and cytoplasmic encapsidated pgRNA were analyzed by Northern blotting. The lower-molecular-weight encapsidated pgRNA species represent the degradation intermediates catalyzed by the RNase activity of HBV pol during viral minus-strand DNA synthesis. HBV precore (p22) and core proteins and FLAG-tagged DDX17 protein were detected by Western blotting. HBV cytoplasmic core DNA was detected by Southern blotting. RC, relaxed circular DNA; SS, single-stranded DNA.

possible effect(s) of DDX17 knockdown on HBV infection in HepG2-NTCP cells, such as viral entry and/or cccDNA transcription, cannot be completely ruled out and, thus, awaits further investigation.

Collectively, the above-described data obtained from different HBV replication systems have demonstrated that DDX17 is a host-intrinsic restriction factor of HBV, which inhibits HBV replication primarily through interrupting pgRNA encapsidation.

DDX17-mediated inhibition of pgRNA encapsidation depends on its RNA-binding activity. As a DEAD box RNA helicase, DDX17 possesses a RNA binding domain and an ATPase domain (22). To identify the functional domain of DDX17 responsible for inhibiting HBV pgRNA encapsidation, two DDX17 mutants were employed (Fig. 6A). Specifically, the DDX17^{K142R} mutation within the ATPase motif of DDX17 inactivates the ATP-binding function and the subsequent ATP hydrolysis activity, and the DDX17^{S277L} mutation alters a SAT sequence, which is considered necessary for the conformational switch essential for

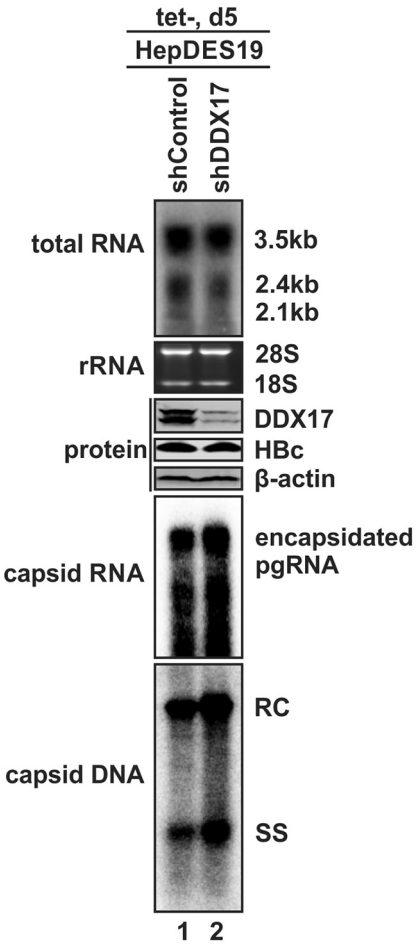

FIG 4 Knockdown of DDX17 promotes HBV pgRNA encapsidation in HBV stable cell line. HBV pgRNA transcription and DNA replication in HepDES19-shControl and HepDES19-shDDX17 cell lines were induced for 5 days after tetracycline (tet) withdrawal. HBV total RNA and cytoplasmic encapsidated pgRNA were analyzed by Northern blotting, HBV core protein and FLAG-tagged DDX17 protein were detected by Western blotting. HBV cytoplasmic core DNA was detected by Southern blotting.

RNA-binding function of helicases (23). Notably, the ATP-binding inactivated mutant DDX17^{K142R} partially attenuated the blockage of HBV pgRNA encapsidation by DDX17 (Fig. 6B, lane 3), and the RNA-binding inactivated mutant DDX17^{S277L} completely abrogated DDX17-mediated inhibition of HBV pgRNA encapsidation (Fig. 6B, lane 4). These results suggest that the RNA-binding activity is pivotal for DDX17 to exert its antiviral activity against HBV.

DDX17 partially gains cytoplasmic localization in the presence of HBV RNA. Previous studies showed that DDX17 is an exportin/importin-dependent nucleocytoplasmic shuttling protein (24). DDX17 is naturally localized in the nucleus but could gain access to cytoplasm after RVFV infection through binding to viral nucleocapsid protein N (17). Considering that HBV pgRNA encapsidation occurs in cytoplasm, DDX17 must gain cytoplasmic localization in the context of HBV replication. To determine the subcellular localization of DDX17, immunofluorescence microscopy was performed on HepG2 cells transfected with FLAG-DDX17 with or without HBV-related plasmids (Fig. 7). In the absence of HBV, DDX17 predominantly exhibited nuclear localization, as indicated by FLAG immunofluorescence (Fig. 7, top), while in the FLAG-DDX17 and pCMVHBV cotransfected cells, some FLAG-staining puncta in the cytoplasm were observed (Fig. 7, middle). Additionally, to examine whether HBV RNA alone can trigger DDX17 subcellular translocation, we cotransfected HepG2 cells with FLAG-DDX17 and pCMVHBVΔORF, which is

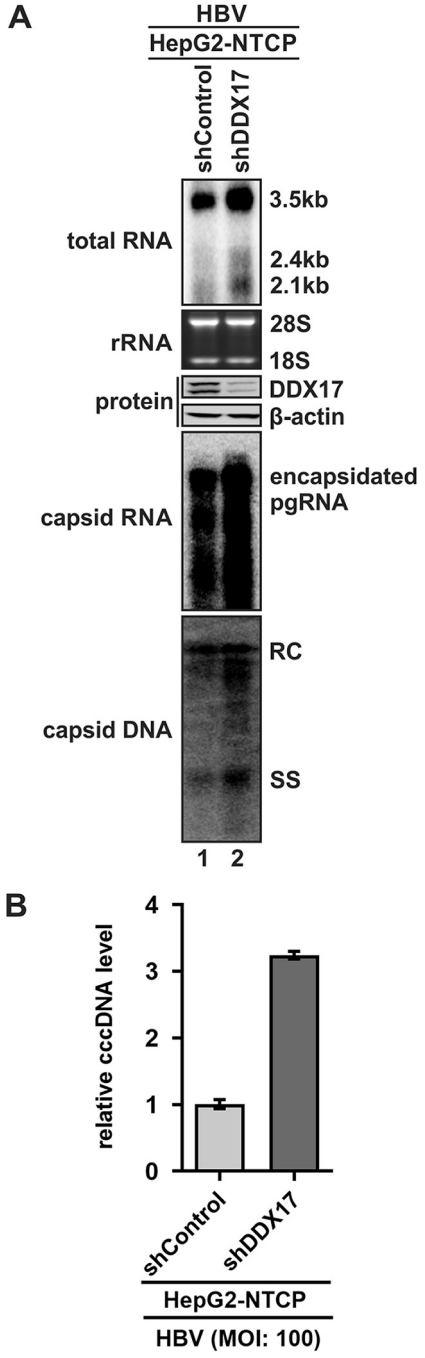

FIG 5 Knockdown of DDX17 promotes HBV infection *in vitro*. HepG2-NTCP-shControl and HepG2-NTCP-shDDX17 cells were infected by HBV at an MOI (multiplicity of infection) of 100 for 9 days. (A) HBV total RNA and cytoplasmic encapsidated pgRNA were analyzed by Northern blotting, and HBV cytoplasmic core DNA was detected by Southern blotting. FLAG-tagged DDX17 proteins were detected by Western blotting. (B) HBV cccDNA was quantified by qPCR and plotted as relative levels of control (fold change of 1) (mean ± standard deviation, $n = 3$).

capable of transcribing HBV RNA but unable to express any viral proteins. Similarly, cytosolic FLAG-staining signal appeared as well in this case (Fig. 7, bottom). Collectively, these data suggest that, in the presence of HBV or even HBV RNA only, DDX17 could be partially translocated from nucleus to cytoplasm together with HBV RNA nuclear export or sequestrated in cytoplasm after protein translation, likely via interacting with HBV RNA.

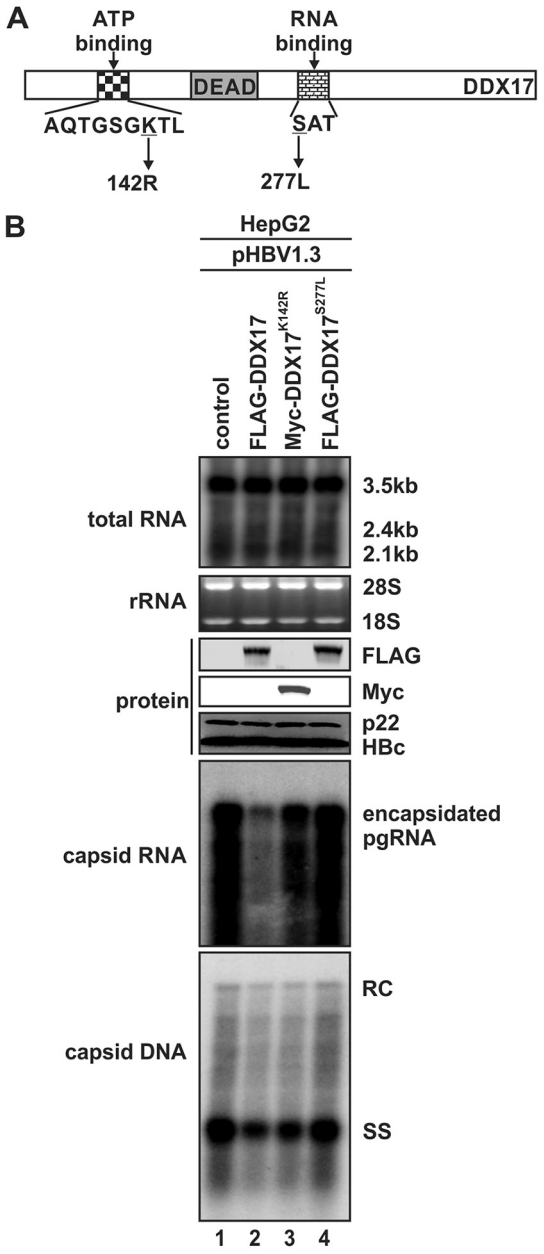

FIG 6 RNA-binding activity is required for DDX17-mediated inhibition of pgRNA encapsidation. (A) Schematic diagram of DDX17. The ATP-binding, RNA-binding, and DEAD domains of DDX17 are indicated by shaded boxes. Point mutations are indicated by the residue number of the wild-type residue and the alteration. (B) HepG2 cells were cotransfected with pHBV1.3 and equal amounts of control vector (lanes 1), FLAG-DDX17 (lanes 2), Myc-DDX17^{K142R} (lanes 3), or FLAG-DDX17^{S277L} (lanes 4). Cells were harvested 5 days posttransfection, followed by Northern and Southern blotting of viral total RNA, encapsidated pgRNA, and core DNA, respectively. HBV precore/core protein and epitope-tagged wild-type and mutant DDX17 protein were analyzed by Western blotting.

DDX17 interacts with HBV RNA intracellularly. To assess the potential interaction between DDX17 and HBV RNA, immunoprecipitation (IP)-Northern blotting was performed. Plasmid FLAG-DDX17, Myc-DDX17^{K142R}, or FLAG-DDX17^{S277L} was coexpressed with pCMVHBV into Huh7 cells. The input HBV RNA was detected by Northern blotting (Fig. 8, top). Western blot detection of wild-type and mutant DDX17 in input and immunoprecipitated samples indicated an efficient protein expression and pulldown of the target proteins. However, HBV pgRNA were detected in the immunoprecipitated samples containing wild-type DDX17, as well as the DDX17^{K142R} mutant to a lesser

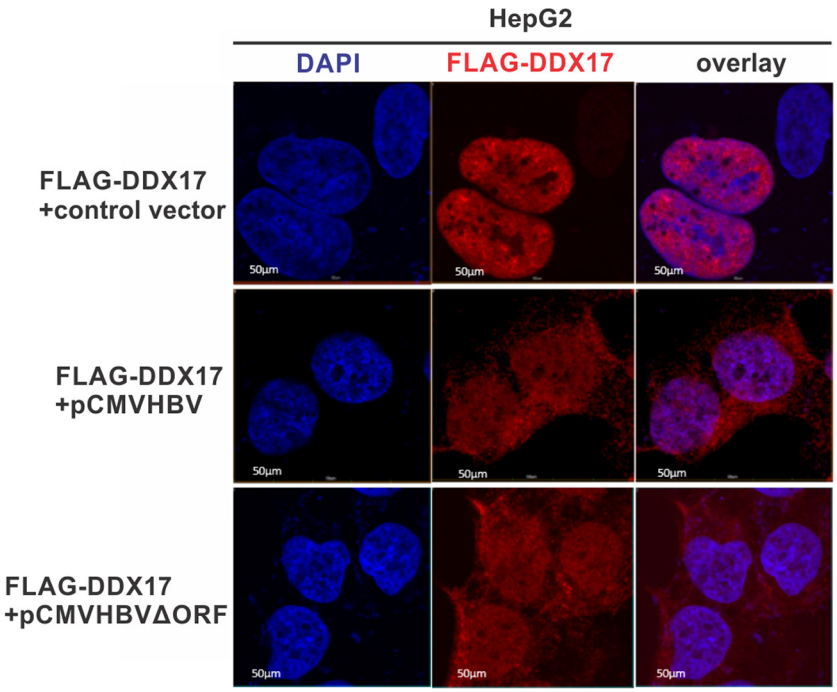

FIG 7 Subcellular localization of DDX17 in the absence and presence of HBV. HepG2 cells were cotransfected with FLAG-DDX17 plus control vector (top), pCMVHBV (middle), or pCMVHBVΔORF (bottom) for 3 days, and the intracellular localization of FLAG-DDX17 was detected by immunofluorescence. Cell nuclei were stained by DAPI.

extent, but not the DDX17^{S277L} mutant (Fig. 8, bottom), suggesting that DDX17 interacts with HBV pgRNA through its RNA-binding motif.

DDX17 interacts with the epsilon of HBV pgRNA. It has been reported that DDX17 restricts Rift Valley fever virus (RVFV) via binding to the stem-loop structures of both viral RNA and host pri-miRNA (17). Our data have demonstrated that DDX17 interacts with HBV pgRNA and inhibits pgRNA encapsidation (Fig. 3 and 8). Given that pgRNA also has a duplicated stem-loop structure, termed epsilon (ε; nucleotides [nt] 1849 to 1909), within both the 5′ and 3′ terminal redundant sequence (nt 1820 to 1918), it is of interest to investigate whether DDX17 interacts with the ε of pgRNA. To this end, a set of pgRNA-expressing plasmids with terminal redundancy deletion was employed, including the 5′ terminal redundancy deletion (Δ5TR), 3′ terminal redundancy deletion (Δ3TR), and the double deletions (Δ3/5TR) (Fig. 9A). The full-length wild type (WT) pgRNA expression plasmid or each of the TR deletion plasmids was transfected into Huh7 cells with or without FLAG-DDX17, followed by IP-Northern blotting. The results demonstrated that the deletion of 3′ TR from pgRNA only slightly reduced the binding with DDX17 compared to that of WT pgRNA (Fig. 9B, lanes 2 and 8); in the absence of 5′ TR, the level of pgRNA coimmunoprecipitated with DDX17 was much lower than that with 3′ TR deletion (Fig. 9B, lanes 4 and 8), whereas with the double TR deletions, no HBV RNA was detected in the DDX17 pulldown sample (Fig. 9B, lane 6). These results indicated that the interaction between DDX17 and HBV pgRNA requires the presence of ε-containing 5′ and 3′ terminal redundant sequences, with the 5′ copy being more indispensable. The preference of 5′ TR binding by DDX17 is in accordance with its antiviral function against pgRNA encapsidation, which employs the ε motif in 5′ TR as a packaging signal (7, 8).

Furthermore, the interactions between DDX17 and ε were validated *in vitro* by electrophoretic mobility shift assay (EMSA). As shown in Fig. 10A, various amounts of purified His-tagged DDX17 or DDX17^{S277L} proteins were incubated with 100 ng ^{32}P-labeled ε RNA, and then the samples were analyzed by gel shift assay. The shifted bands

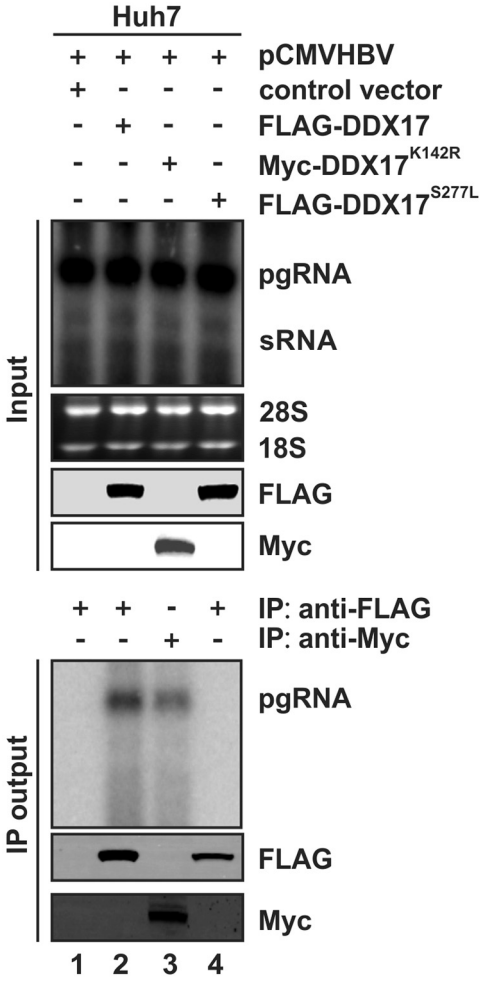

FIG 8 DDX17 interacts with HBV RNA in cells. Huh7 cells were cotransfected with pCMVHBV and control vector (lane 1), FLAG-DDX17 (lane 2), Myc-DDX17^{K142R} (lanes 3), or FLAG-DDX17^{S277L} (lane 4) for 4 days. (Top) The input HBV RNA and epitope-tagged DDX17 proteins were detected by Northern blotting and Western blotting, respectively. Cell lysates were immunoprecipitated by beads coated with anti-FLAG or anti-Myc antibodies. (Bottom) The immunoprecipitated FLAG-DDX17, Myc-DDX17^{K142R}, and FLAG-DDX17^{S277L} were detected by Western blotting. HBV RNA captured by beads was extracted and subjected to Northern blotting.

indicated the formation of DDX17-ε ribonucleoprotein complex, and the intensity of shifted bands was increased in a DDX17 dose-dependent manner. However, ε RNA band shift was not detected in the case of RNA binding-deficient mutant DDX17^{S277L}. In addition, the binding of DDX17 with ε RNA was further confirmed by super shifting assay with add-on anti-His antibody (Fig. 10B, lanes 4, 6, and 8) and by competitive EMSA with nonradiolabeled ε (Fig. 10B, lanes 9 to 11). Collectively, these data clearly suggested that DDX17 interacts with pgRNA via the ε stem-loop sequence.

DDX17 competes with HBV pol for binding to pgRNA in cell cultures. During HBV replication, viral pol binds to the 5′ ε of pgRNA and triggers the encapsidation of pgRNA (7, 8). Given that DDX17 inhibits pgRNA encapsidation and that it also binds to pgRNA via the ε motif, it is plausible that DDX17 competes with pol for binding to pgRNA and, thus, inhibits pgRNA encapsidation. To test this hypothesis, fixed amounts of FLAG-pol and pCMVHBVΔCΔP were cotransfected into Huh7 cells together with increased amounts of hemagglutinin (HA)-DDX17, followed by immunoprecipitation (IP)-Northern blotting. Indeed, with the increased levels of HA-DDX17 expression, the levels of DDX17-bound pgRNA increased together with decreased levels of pol-bound pgRNA in a dose-dependent manner (Fig. 11). Based on the results from this study, we

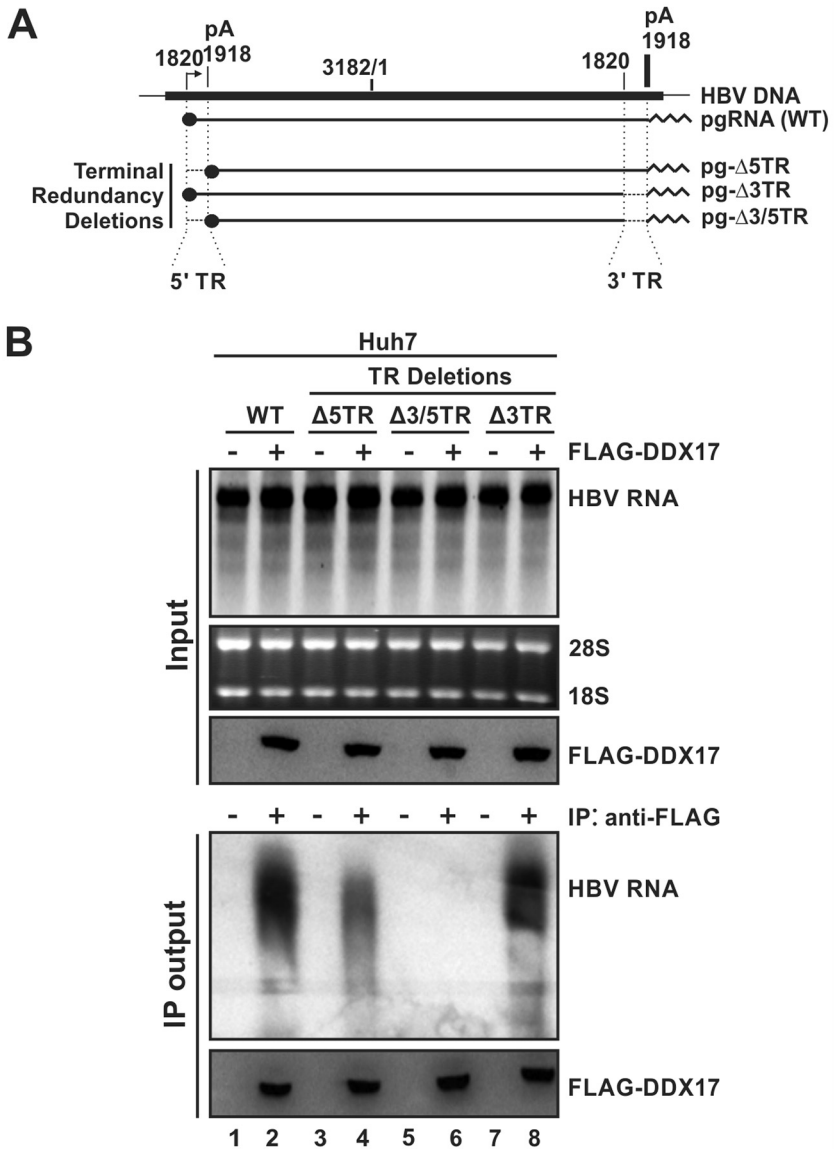

FIG 9 HBV pgRNA sequence element responsible for DDX17 binding is located in the terminal redundancy. (A) Diagram of HBV plasmid constructs expressing the full-length wild-type (WT) pgRNA and mutant pgRNA with terminal redundancy (TR) deletions, including the 5′ TR deletion mutant (pg-Δ5TR), 3′ TR deletion mutant (pg-Δ3TR), and double-deletion mutant (pg-Δ3/5TR). The arrow indicates the pgRNA transcription initiation site (nt 1820). pA is the polyadenylation signal (nt 1918). The solid dot indicates the 5′ cap of mRNA, and the sawtooth line represents the poly(A) tail. The 5′ and 3′ TR (nt 1820 to 1918) are indicated. (B) Huh7 cells were transfected with the indicated plasmids for 4 days. (Top) The input HBV RNA and FLAG-tagged DDX17 proteins were detected by Northern blotting and Western blotting, respectively. Cell lysates were immunoprecipitated by beads coated with anti-FLAG antibodies. (Bottom) The immunoprecipitated FLAG-DDX17 was detected by Western blotting. HBV RNA captured by beads were extracted and subjected to Northern blotting.

can conclude that DDX17 competes with pol to bind to the 5′ ε of HBV pgRNA, which results in inhibition of pgRNA encapsidation and thereby the subsequent DNA replication.

DISCUSSION

The helicase proteins specify a large number of motor enzymes that use energy derived from NTP hydrolysis to unwind or rewind the double-stranded nucleic acids (DNA, RNA, or DNA-RNA hybrid) (25). DDX17, a member of the DEAD box RNA helicase family proteins, plays pleiotropic roles in cellular RNA processing and metabolism,

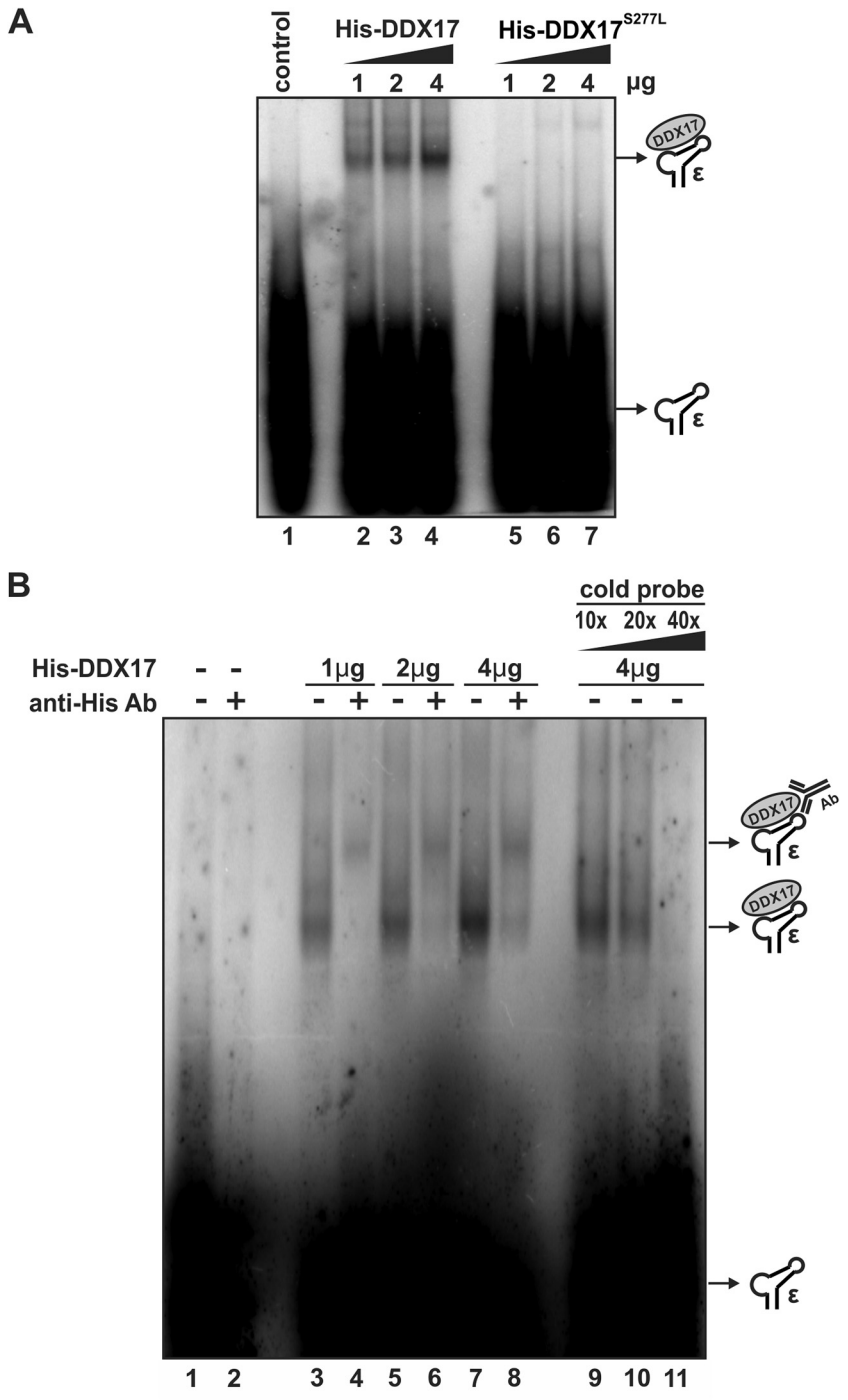

FIG 10 DDX17 binds to ε RNA *in vitro*. (A) Indicated amounts of purified His-tagged DDX17 or DDX17^{S277L} proteins were incubated with 100 ng ^{32}P-labeled ε RNA in binding buffer to form nucleoprotein complexes. The samples were analyzed by native PAGE, and the shifted bands were detected by autoradiography (lanes 2 to 7). Probe only served as a negative control (lane 1). (B) Indicated amounts of purified His-tagged DDX17 proteins were incubated with 100 ng ^{32}P-labeled ε RNA in binding buffer to form His-DDX17/ε complexes (lanes 3, 5, and 7). Monoclonal anti-His antibody was used to bind the His-DDX17/ε complex for supershifting (lanes 4, 6, and 8). Excessive amounts (10×, 20×, and 40×) of cold unlabeled ε RNA were used to compete with the ^{32}P-labeled ε RNA for DDX17 binding (lanes 9 to 11). Probe only and probe mixed with anti-His antibody served as negative controls (lanes 1 and 2). The samples were separated by native PAGE and subjected to autoradiography.

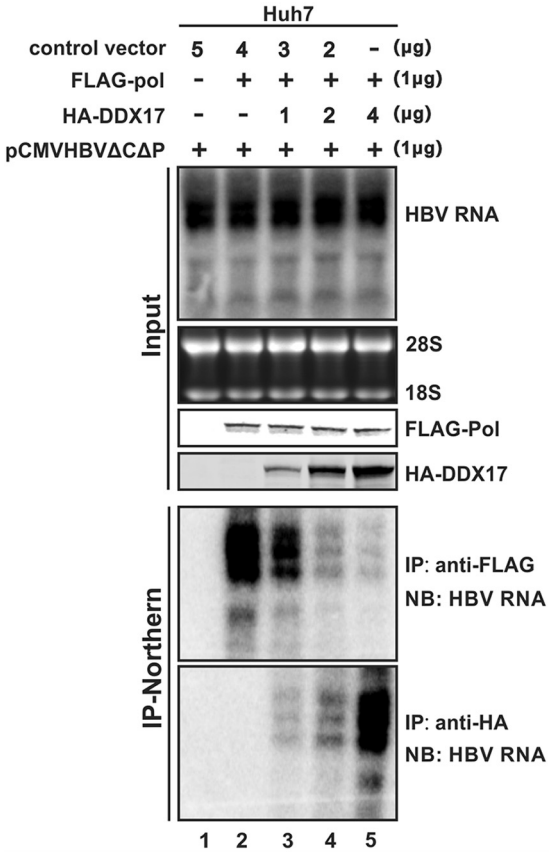

FIG 11 DDX17 competes with HBV pol for binding to pgRNA in cell cultures. Huh7 cells in 60-mm dishes were transfected with 1 μg of pCMVHBVΔCΔP and 5 μg control vector (lane 1) or 1 μg of FLAG-Pol plus increased amounts of HA-DDX17 (0 μg, 1 μg, 2 μg, and 4 μg; lanes 2 to 5). Control vector was supplemented to normalize the total amount of transfected plasmids to 6 μg per transfection. Cells were harvested 5 days posttransfection. (Top) The input HBV RNA, FLAG-pol, and HA-DDX17 proteins were detected by Northern and Western blotting, respectively. Cell lysates were immunoprecipitated by beads coated with anti-FLAG or anti-HA antibodies. (Bottom) The immunoprecipitated HBV RNA were extracted and analyzed by Northern blotting.

including miRNA biogenesis, mRNA folding, splicing, translation, and stability, etc., which, in turn, directly and/or indirectly regulates cellular homeostasis and oncogenesis signaling pathways (16, 22, 26–28). In addition to cellular RNA, there is a growing body of evidence showing that cellular DDX17 also exerts regulatory effects on viral RNA molecules in virus-infected cells, either proviral or antiviral effects (29). For example, it has been reported that DDX17 is required for efficient RNA synthesis of H1N1 and H5N1 avian influenza viruses (30) and that DDX17 promotes the production of HIV-1 infectious particles by modulating viral genomic RNA packaging and the frameshift of Gag-Pol translation (20). The antiviral effect of DDX17 has been reported in RVFV-infected cells, which involves both endogenous miRNA biogenesis and surveillance against structured non-self viral RNA elements; the latter is a DDX17-mediated binding and unwinding of two primary noncoding stem-loop structures of the small segment of RVFV RNA genomes (17, 31). Furthermore, the plant DDX17-like RH30 DEAD box helicase has been shown to inhibit tombusviruses primarily through binding to the structured *cis*-acting elements of viral RNA and blocking the assembly of viral replication complex (32). These studies demonstrated that DDX17 exhibits a broad species and tissue distribution as well as broad proviral/antiviral spectrum. In this study, we further demonstrated that the hepatic DDX17 possesses antiviral activity against HBV.

HBV is a small DNA virus that replicates its genome via reverse transcription of pgRNA in viral capsid; therefore, host factors/functions targeting pgRNA stability and

encapsidation ought to pose significant influences on HBV DNA replication (6). We have previously identified ZAP as an intrinsic host restriction factor that promotes HBV RNA decay (11). Furthermore, it has been reported that DDX17 serves as a cofactor of ZAP to promote ZAP-mediated degradation of Moloney murine leukemia virus (MLV) RNA in HEK293T cells (15). Therefore, in this study, we attempted to assess the potential role of DDX17 in ZAP-mediated HBV RNA degradation. However, an efficient knockdown of DDX17 did not markedly affect the steady-state level of HBV RNA with or without ZAP overexpression, indicating that DDX17 is not or at least is not absolutely required for ZAP's anti-HBV activity (Fig. 2). While there may be a cell type- or virus-specific requirement of DDX17 for ZAP-mediated RNA degradation, another possibility is that the residual level of DDX17 after knockdown is sufficient to potentiate ZAP activity. Nonetheless, our study clearly uncovered a novel anti-HBV function of DDX17 beyond RNA degradation, which is that DDX17 inhibits HBV pgRNA encapsidation, an essential step prior to viral reverse transcription. In the HBV transient and stable transfection cell culture systems, DDX17 ectopic expression or knockdown significantly reduced or upregulated pgRNA encapsidation and subsequent DNA replication, respectively, without affecting the total pgRNA level and core protein expression, suggesting that DDX17 inhibits HBV replication primarily by blocking pgRNA encapsidation (Fig. 3 and 4). The antiviral activity of DDX17 was further confirmed in HBV-infected HepG2-NTCP cells upon stable knockdown of DDX17, but compared to HBV transfection systems, the upregulation of pgRNA encapsidation might result in an overall increase of HBV DNA, cccDNA, and total RNA along the virus replication cycle in infection systems (Fig. 5). However, it is worth noting that the intracellular cccDNA amplification was found to be less efficient in NTCP-reconstituted hepatoma cells (33–36). Thus, whether DDX17 possesses any additional effect(s) on cccDNA formation and/or transcription requires further investigation.

Consistent with the ATP-dependent RNA helicase activity of DDX17, both the RNA-binding and ATP-binding mutant forms of DDX17 significantly diminished its antiviral activity against HBV, and the RNA-binding motif of DDX17 appears more important for its antiviral activity than the ATP-binding motif (Fig. 6). In line with this, we have obtained multiple lines of evidence to support an interaction between DDX17 and HBV pgRNA. First, HBV RNA alone could induce the cytoplasmic localization of DDX17 (Fig. 7), although whether this is due to HBV RNA-mediated DDX17 nuclear-cytoplasmic translocation or cytoplasmic retention of nascent DDX17 remains unclear. Second, IP-Northern blot assay revealed that DDX17, but not the RNA-binding deficient mutant DDX17^{S277L}, interacts with pgRNA in cell cultures (Fig. 8). Furthermore, the HBV RNA sequence element responsible for DDX17 binding is predominantly located in the 5′ terminal redundancy (TR) region, which contains the stem-loop structure ε. Interestingly, DDX17 binds to 3′ TR much less efficiently than the 5′ counterpart despite the fact that their sequences are identical (Fig. 9B). Such discrepancy is perhaps due to the different surrounding ribonucleotide sequences of 5′ and 3′ TR and their associated proteins/factors, for example, the 5′ cap structure and 3′ poly(A) tail of pgRNA, which may influence the binding of DDX17. In line with this notion, the 5′ cap upstream of ε is essential for HBV pgRNA encapsidation (37).

In addition, the gel shift assay clearly demonstrated that DDX17 can directly bind to ε *in vitro* in an RNA-binding motif-dependent manner (Fig. 10). The binding of DDX17 with HBV ε stem-loop structure is consistent with DEAD box helicases recognizing RNA substrate in a structure-dependent manner (29).

Serving as the packaging signal for HBV pgRNA, the ε stem-loop interacts with pol to form ribonucleoprotein complex, which, in turn, is encapsulated into viral capsid for reverse transcription to take place (7). In this regard, we found that the binding of DDX17 to ε competes with pol-ε interaction in cell cultures (Fig. 11), which would lead to the blockage of pgRNA encapsidation. Mechanistically, it is also plausible that DDX17 unwinds or rearranges the structure of ε with its ATP-dependent helicase activity or functions as an RNA clamp to arrest the dynamic changes of ε structure. The

latter may explain why the ATPase-deficient mutant DDX17^{K142R} retains partial antiviral activity against pgRNA encapsidation (Fig. 6).

Besides RNA binding activity, DDX17 is also able to interact with counterpart proteins and ribonucleoproteins to regulate various host and viral functions (29, 38). Whether there are host and/or viral cofactors involved in DDX17-ε interaction and the inhibition of pgRNA encapsidation awaits further investigation. Among the DDX17-interacting proteins, it is worth noting that DDX5 is a paralog of DDX17 and both helicases exert overlapping or cooperative functions to regulate cellular gene transcription, splicing, and miRNA biogenesis (26, 39). However, in terms of virus-host interaction, DDX17 and DDX5 may work differently, although the two helicases can form a heterodimer. For example, DDX5 does not play a role in regulating HIV-1 and RVFV infection similar to that of DDX17 (17, 20). It has been reported that DDX5 epigenetically represses HBV cccDNA transcription through interacting with the long noncoding RNA HOTAIR in complex with polycomb repressive complex 2 (PRC2) (40). Thus, it is of interest to systematically assess and compare the potential antiviral effect of DDX5 and DDX17 on HBV transcription and pgRNA encapsidation in a future study.

The stem-loop structure ε of pgRNA represents a unique non-self signature in HBV-infected cells, which is a hot spot of virus-host interactions. A few host proteins have been identified as ε-binding factors in previous studies, including ZAP and ISG20 RNase, which degrade HBV RNA (11, 41), RNA-binding motif protein 24 (RBM24), which promotes pol-ε binding and pgRNA encapsidation (42), and RNA helicase RIG-I, which blocks pgRNA encapsidation and induces type III interferons (43). In the current study, we identified DDX17 as a novel ε-binding factor that competes with pol-ε binding to prevent pgRNA encapsidation. Considering that multiple factors could bind to ε to perform diverse functions, it is of great interest to investigate the spatiotemporal and functional relationship between these ε-binding proteins in the context of HBV infection, which will lead to a more coherent understanding of virus-host interaction around HBV ε. On the other hand, the interplay between ε and binding proteins can also be exploited to develop novel antiviral means for treatment of HBV infection.

MATERIALS AND METHODS

Cell lines. HepG2, Huh7, and HEK293T cells were maintained in Dulbecco's modified Eagle medium (DMEM)-F12 medium (Corning) supplemented with 10% fetal bovine serum, 100 U/ml penicillin, and 100 μg/ml streptomycin. HepDES19 cells were maintained in the same medium with addition of 1 μg/ml tetracycline (tet) and 400 μg/ml G418 (44). To initiate HBV replication in HepDES19 cells, tet was withdrawn from the culture medium and the cells were cultured for the indicated time period. The HepG2-NTCP cell line, supporting HBV infection, was maintained as described previously (45). To establish HepDES19 and HepG2-NTCP cells with stable DDX17 knockdown (shDDX17) and control knockdown (shControl), the cells were transduced by DDX17 short hairpin RNA (shRNA) and control shRNA lentiviral particles (Santa Cruz Biotechnology), respectively, per the manufacturer's directions. The transduced cells were selected with 3 μg/ml puromycin, and the antibiotic-resistant cells were pooled and expanded into cell lines. Primary human hepatocytes (PHH) were obtained from the Biospecimen Repository and Processing Core of Pittsburgh Liver Research Center. Recombinant human IFN-α2a was purchased from PBL Biomedical Laboratories.

Plasmids and transfection. HBV (genotype D, subtype ayw) replication-competent plasmids, pHBV1.3 and pCMVHBV, in which the transcription of viral pgRNA is governed by authentic HBV core promoter and the human cytomegalovirus immediate-early (CMV-IE) promoter, respectively, were described previously (46). Plasmid pCMVHBVΔCΔP harbors start codon mutations of core (ATG to CTG) and pol (ATG to ACG) ORF in the pCMVHBV backbone to block the expression of core and pol (41). Plasmid pCMVHBVΔORF contains additional stop codon mutations in S ORF (T218A/T221A) and X ORF (C1397T), introduced by site-directed mutagenesis, which only supports HBV RNA transcription without translation of viral proteins. HBV pgRNA terminal redundancy (TR) deletion clones (pg-Δ5TR, pg-Δ3TR, and pg-Δ5/3TR) were constructed previously (11). Plasmid pCMV-FLAG-pol, expressing the N-terminally 3×FLAG-tagged pol, was a gift from Wang-Shick Ryu (47). Plasmid FLAG-DDX17, expressing wild-type DDX17 (p72) with FLAG tag at the N terminus and plasmid Myc-DDX17^{K142R} expressing a Myc-tagged DDX17 with K142R mutation in the ATPase motif, were kindly provided by Didier Auboeuf and Cyril Bourgeois (26, 39, 48). Plasmid FLAG-DDX17^{S277L} expresses a Flag-tagged DDX17 with S277L mutation in the helicase motif to block RNA binding, which was constructed by introducing S277L mutation into plasmid FLAG-DDX17 through site-directed mutagenesis. Plasmid HA-DDX17 expressing wild-type DDX17 with an N-terminal HA tag was constructed by cloning the DDX17 ORF into the EcoRI/XhoI restriction sites in expression vector pCMV-HA-N (Clontech). Plasmid ZAP-S, expressing the short isoform of human ZAP with an N-terminal HA tag, was a gift from Harmit Malik (49). Cells were transfected with

the indicated plasmid(s) by Lipofectamine 2000 (Life Technologies) according to the manufacturer's directions.

HBV infection. HepG2-NTCP-shControl and HepG2-NTCP-shDDX17 cells were inoculated with HepDE19-derived HBV virion particles at 100 virus genome equivalents (vge)/cell according to a published protocol (45).

HBV nucleic acid analyses. Total cellular HBV RNA, cytoplasmic encapsidated HBV pgRNA, and core DNA were extracted and subjected to Northern and Southern blotting as described previously (41). Hybridization signals were recorded on a phosphorimager screen and scanned by the Typhoon FLA-7000 imager (GE Healthcare). HBV cccDNA was extracted by a modified Hirt DNA extraction method and quantified by quantitative PCR (qPCR) according to previously published protocols (45, 50).

Western blot assay. Whole-cell lysate samples prepared in Laemmli buffer were resolved in 4% to 12% gradient SDS-PAGE, and proteins were transferred onto Immobilon PVDF-FL membrane (Millipore). The membranes were blocked with Western Breeze blocking buffer (Life Technologies) and blotted with antibodies against FLAG tag (clone M2; Sigma), Myc-tag (Santa Cruz), HA tag (clone 16B12; Covance), DDX17 (Santa Cruz), ISG56 (Santa Cruz), β-actin (Millipore), and HBV precore/core (51), as indicated. Bound antibodies were revealed by IRDye secondary antibodies. The immunoblot signals were visualized and quantified with the Li-COR Odyssey system.

Immunofluorescence. HepG2 cells were transfected with FLAG-DDX17 alone or cotransfected with FLAG-DDX17 and plasmid pCMVHBV or pCMVHBVΔORF for 48 h, followed by fixation with 4% paraformaldehyde and permeabilization of the cell membrane with 0.2% Triton X-100. Cells were then stained with anti-FLAG antibodies (clone 16B12; Covance), and the bound antibodies were visualized by Alexa Fluor 594 goat anti-mouse IgG (Life Technologies). Nuclei were counterstained with 4′,6-diamidino-2-phenylindole (DAPI). Cells were imaged with a Nikon fluorescence microscope and photographed with a charge-coupled device camera.

DDX17 and HBV RNA coimmunoprecipitation. Huh7 cells were transfected with the indicated plasmids and maintained for 4 days. The harvested cells were lysed on ice with cell lysis buffer containing 1% NP-40, 10 mM Tris-HCl (pH 7.5), 1 mM EDTA, 50 mM NaCl, 8% sucrose, and 1 U/μl of RNasin plus RNase inhibitor (Promega). After centrifugation to remove the cell debris, the clarified cell lysates were incubated with EZview red anti-Myc, anti-HA, or anti-FLAG affinity gel (Sigma-Aldrich) at 4°C for 2 h with gentle rotation. The beads were spun down and resuspended gently with rinse buffer (10 mM Tris-HCl [pH 7.5], 1 mM EDTA, 50 mM NaCl, and 1 U/μl of RNasin Plus RNase inhibitor) three times at 4°C. The pelleted beads were subjected to RNA extraction with TRIzol and protein sample preparation with Laemmli buffer. Immunoprecipitated protein and HBV RNA were analyzed by Western and Northern blot assays, respectively.

Recombinant His-DDX17 protein expression and purification. The ORF of wild-type DDX17 and DDX17^{S277L} mutant were PCR amplified from plasmid FLAG-DDX17 and FLAG-DDX17^{S277L}, respectively, and cloned into pRSET, a prokaryotic expression vector (Thermo Fisher Scientific) under the T7 promoter at BamHI and EcoRI sites to generate plasmid expressing His-tagged DDX17 (His-DDX17) and DDX17^{S277L} (His-DDX17^{S277L}). The protein expression vectors were transformed into *Escherichia coli* BL21(DE3) pLysS competent cells (Promega), and the cells were propagated with aeration at 37°C in 0.5 liters of SOB broth in the presence of 100 μg/ml ampicillin to an A_{600} of ~0.6, followed by adding 1 mM isopropyl-1-thio-β-D-galactopyranoside (IPTG) to induce protein expression at 37°C for 3 h. The induction of recombinant proteins was confirmed by SDS-PAGE and Coomassie staining compared to an uninduced control sample.

The aforementioned His-tagged proteins expressed from bacteria were purified using denaturing conditions. Briefly, the bacterial pellet was resuspended in 0.1 M Na-phosphate, 0.1 M Tris-HCl, 6 M guanidine-HCl, pH 8.0 with fresh 1 mM phenylmethylsulfonyl fluoride (PMSF) and stirred for 2 h at 4°C to lyse the cells and solubilize the proteins under denaturing conditions. The cell extract was centrifuged at 12,000 $\times$ *g* for 20 min. The supernatant fraction containing soluble protein was incubated in batch with PerfectPro nickel-nitrilotriacetic acid (Ni-NTA) agarose (5PRIME) for 1 h at room temperature. The resin was washed once with 0.1 M Na-phosphate, 0.1 M Tris-HCl, 6 M guanidine-HCl, pH 6.3, and two times with 0.1 M Na-phosphate, 0.1 M Tris-HCl, 6 M guanidine-HCl, pH 6.3, with an additional 20 mM imidazole. The resin was loaded into the supplied purification column, and the protein was eluted with 0.1 M Na-phosphate, 0.1 M Tris-HCl, 6 M guanidine-HCl, pH 4.6, and 300 mM imidazole with 1 mM PMSF. The eluted protein was dialyzed against three changes of 1$\times$ phosphate-buffered saline (PBS), 300 mM NaCl, 5% glycerol with freshly added 1 mM dithiothreitol (DTT) and 0.1 mM PMSF. The soluble proteins were concentrated with Pierce concentrators (9-kDa cutoff; Thermo Scientific). Bio-Rad Bradford protein assay and Coomassie staining were used to measure the concentration and the purity of the proteins.

EMSA. The synthetic HBV ε RNA fragments (nt 1847 to 1911) were dissolved in diethyl pyrocarbonate-treated 1$\times$ Tris-EDTA buffer to a concentration of 1 μg/μl and denatured in a 80°C water bath for 5 min, followed by slow cooling to room temperature for RNA annealing and secondary structure formation. HBV ε RNA was 5′ γ-^{32}P-radiolabeled by T4 polynucleotide kinase (New England Biolabs) and purified by a Quick Spin Sephadex G25 column (Roche) as previously described (41).

The indicated amounts of wild-type and mutant DDX17 proteins were incubated with 100 ng ^{32}P-radiolabeled HBV ε RNA in the presence of 20 mM HEPES, 100 mM KCl, 1 mM DTT, 0.5 mg/ml bovine serum albumin, 10% glycerol, and 0.05 μg/μl nonspecific competitor RNA poly(dI-dC) at 30°C for 30 min to form ribonucleoprotein complexes; 1 μl of monoclonal anti-polyhistidine antibody (clone H1029; Sigma) was used for supershifting of the His-DDX17/HBV ε complex; 1 μg, 2 μg, or 4 μg of cold unlabeled HBV ε RNA was used to compete for binding of the DDX17 protein to 100 ng radiolabeled HBV ε. The ribonucleoprotein complexes were separated by native 5% PAGE at 200 V in a gel buffer containing 50 mM

Tris, 45 mM boric acid, 1% (vol/vol) glycerol for 2 h in a cold room. The gel was fixed in 10% acetic acid and 10% methanol, dried, and visualized by autoradiography.

ACKNOWLEDGMENTS

We thank Didier Auboeuf and Cyril Bourgeois (INSERM, France) for providing plasmids FLAG-DDX17 and Myc-DDX17^{K142R}, Harmit Malik (Fred Hutchinson Cancer Research Center) for providing plasmid HA-ZAP-S, and Wang-Shick Ryu (Yonsei University, South Korea) for providing plasmid pCMV-FLAG-pol.

This study was partly supported by the U.S. National Institutes of Health (R01AI110762, R01AI134818, and R01AI150255 to H.G.; P30DK12053 to Pittsburgh Liver Research Center [PLRC]) and the National Natural Science Foundation of China (81670528 to R.M. and J.Z.).

REFERENCES

1. Revill PA, Chisari FV, Block JM, Dandri M, Gehring AJ, Guo H, Hu J, Kramvis A, Lampertico P, Janssen HLA, Levrero M, Li W, Liang TJ, Lim SG, Lu F, Penicaud MC, Tavis JE, Thimme R, Zoulim F, Members of the ICE-HBV Working Groups, ICE-HBV Stakeholders Group Chairs, ICE-HBV Senior Advisors. 2019. A global scientific strategy to cure hepatitis B. Lancet Gastroenterol Hepatol 4:545–558. https://doi.org/10.1016/S2468-1253(19)30119-0.
2. Block TM, Guo H, Guo JT. 2007. Molecular virology of hepatitis B virus for clinicians. Clin Liver Dis 11:685–706. https://doi.org/10.1016/j.cld.2007.08.002.
3. Seeger C, Mason WS. 2000. Hepatitis B virus biology. Microbiol Mol Biol Rev 64:51–68. https://doi.org/10.1128/MMBR.64.1.51-68.2000.
4. Yan H, Zhong G, Xu G, He W, Jing Z, Gao Z, Huang Y, Qi Y, Peng B, Wang H, Fu L, Song M, Chen P, Gao W, Ren B, Sun Y, Cai T, Feng X, Sui J, Li W. 2012. Sodium taurocholate cotransporting polypeptide is a functional receptor for human hepatitis B and D virus. Elife 1:e00049. https://doi.org/10.7554/eLife.00049.
5. Marchetti AL, Guo H. 2020. New insights on molecular mechanism of hepatitis B virus covalently closed circular DNA formation. Cells 9:2430. https://doi.org/10.3390/cells9112430.
6. Mitra B, Thapa RJ, Guo H, Block TM. 2018. Host functions used by hepatitis B virus to complete its life cycle: implications for developing host-targeting agents to treat chronic hepatitis B. Antiviral Res 158:185–198. https://doi.org/10.1016/j.antiviral.2018.08.014.
7. Hu J, Seeger C. 2015. Hepadnavirus genome replication and persistence. Cold Spring Harb Perspect Med 5:a021386. https://doi.org/10.1101/cshperspect.a021386.
8. Nassal M. 2008. Hepatitis B viruses: reverse transcription a different way. Virus Res 134:235–249. https://doi.org/10.1016/j.virusres.2007.12.024.
9. Liu S, Zhou B, Valdes JD, Sun J, Guo H. 2019. Serum hepatitis B virus RNA: a new potential biomarker for chronic hepatitis B virus infection. Hepatology 69:1816–1827. https://doi.org/10.1002/hep.30325.
10. Hu J, Liu K. 2017. Complete and incomplete hepatitis B virus particles: formation, function, and application. Viruses 9:56. https://doi.org/10.3390/v9030056.
11. Mao R, Nie H, Cai D, Zhang J, Liu H, Yan R, Cuconati A, Block TM, Guo JT, Guo H. 2013. Inhibition of hepatitis B virus replication by the host zinc finger antiviral protein. PLoS Pathog 9:e1003494. https://doi.org/10.1371/journal.ppat.1003494.
12. Gao G, Guo X, Goff SP. 2002. Inhibition of retroviral RNA production by ZAP, a CCCH-type zinc finger protein. Science 297:1703–1706. https://doi.org/10.1126/science.1074276.
13. Guo X, Carroll JW, Macdonald MR, Goff SP, Gao G. 2004. The zinc finger antiviral protein directly binds to specific viral mRNAs through the CCCH zinc finger motifs. J Virol 78:12781–12787. https://doi.org/10.1128/JVI.78.23.12781-12787.2004.
14. Guo X, Ma J, Sun J, Gao G. 2007. The zinc-finger antiviral protein recruits the RNA processing exosome to degrade the target mRNA. Proc Natl Acad Sci U S A 104:151–156. https://doi.org/10.1073/pnas.0607063104.
15. Chen G, Guo X, Lv F, Xu Y, Gao G. 2008. p72 DEAD box RNA helicase is required for optimal function of the zinc-finger antiviral protein. Proc Natl Acad Sci U S A 105:4352–4357. https://doi.org/10.1073/pnas.0712276105.
16. Linder P, Jankowsky E. 2011. From unwinding to clamping–the DEAD box RNA helicase family. Nat Rev Mol Cell Biol 12:505–516. https://doi.org/10.1038/nrm3154.
17. Moy RH, Cole BS, Yasunaga A, Gold B, Shankarling G, Varble A, Molleston JM, tenOever BR, Lynch KW, Cherry S. 2014. Stem-loop recognition by DDX17 facilitates miRNA processing and antiviral defense. Cell 158:764–777. https://doi.org/10.1016/j.cell.2014.06.023.
18. Uhlmann-Schiffler H, Rossler OG, Stahl H. 2002. The mRNA of DEAD box protein p72 is alternatively translated into an 82-kDa RNA helicase. J Biol Chem 277:1066–1075. https://doi.org/10.1074/jbc.M107535200.
19. Geißler V, Altmeyer S, Stein B, Uhlmann-Schiffler H, Stahl H. 2013. The RNA helicase Ddx5/p68 binds to hUpf3 and enhances NMD of Ddx17/p72 and Smg5 mRNA. Nucleic Acids Res 41:7875–7888. https://doi.org/10.1093/nar/gkt538.
20. Lorgeoux RP, Pan Q, Le Duff Y, Liang C. 2013. DDX17 promotes the production of infectious HIV-1 particles through modulating viral RNA packaging and translation frameshift. Virology 443:384–392. https://doi.org/10.1016/j.virol.2013.05.026.
21. Zhu Y, Gao G. 2008. ZAP-mediated mRNA degradation. RNA Biol 5:65–67. https://doi.org/10.4161/rna.5.2.6044.
22. Bourgeois CF, Mortreux F, Auboeuf D. 2016. The multiple functions of RNA helicases as drivers and regulators of gene expression. Nat Rev Mol Cell Biol 17:426–438. https://doi.org/10.1038/nrm.2016.50.
23. Honig A, Auboeuf D, Parker MM, O'Malley BW, Berget SM. 2002. Regulation of alternative splicing by the ATP-dependent DEAD-box RNA helicase p72. Mol Cell Biol 22:5698–5707. https://doi.org/10.1128/MCB.22.16.5698-5707.2002.
24. Li K, Mo C, Gong D, Chen Y, Huang Z, Li Y, Zhang J, Huang L, Li Y, Fuller-Pace FV, Lin P, Wei Y. 2017. DDX17 nucleocytoplasmic shuttling promotes acquired gefitinib resistance in non-small cell lung cancer cells via activation of beta-catenin. Cancer Lett 400:194–202. https://doi.org/10.1016/j.canlet.2017.02.029.
25. Wu Y. 2012. Unwinding and rewinding: double faces of helicase? J Nucleic Acids 2012:140601. https://doi.org/10.1155/2012/140601.
26. Dardenne E, Polay Espinoza M, Fattet L, Germann S, Lambert MP, Neil H, Zonta E, Mortada H, Gratadou L, Deygas M, Chakrama FZ, Samaan S, Desmet FO, Tranchevent LC, Dutertre M, Rimokh R, Bourgeois CF, Auboeuf D. 2014. RNA helicases DDX5 and DDX17 dynamically orchestrate transcription, miRNA, and splicing programs in cell differentiation. Cell Rep 7:1900–1913. https://doi.org/10.1016/j.celrep.2014.05.010.
27. Fuller-Pace FV. 2013. The DEAD box proteins DDX5 (p68) and DDX17 (p72): multi-tasking transcriptional regulators. Biochim Biophys Acta 1829:756–763. https://doi.org/10.1016/j.bbagrm.2013.03.004.
28. Wu KJ. 2020. The role of miRNA biogenesis and DDX17 in tumorigenesis and cancer stemness. Biomed J 43:107–114. https://doi.org/10.1016/j.bj.2020.03.001.
29. Taschuk F, Cherry S. 2020. DEAD-box helicases: sensors, regulators, and effectors for antiviral defense. Viruses 12:181. https://doi.org/10.3390/v12020181.
30. Bortz E, Westera L, Maamary J, Steel J, Albrecht RA, Manicassamy B, Chase G, Martinez-Sobrido L, Schwemmle M, Garcia-Sastre A. 2011. Host- and strain-specific regulation of influenza virus polymerase activity by interacting cellular proteins. mBio 2:e00151-11. https://doi.org/10.1128/mBio.00151-11.
31. Nelson CR, Mrozowich T, Park SM, D'Souza S, Henrickson A, Vigar JRJ, Wieden HJ, Owens RJ, Demeler B, Patel TR. 2020. Human DDX17 unwinds rift valley fever virus non-coding RNAs. Int J Mol Sci 22:54. https://doi.org/10.3390/ijms22010054.
32. Wu CY, Nagy PD. 2019. Blocking tombusvirus replication through the antiviral functions of DDX17-like RH30 DEAD-box helicase. PLoS Pathog 15:e1007771. https://doi.org/10.1371/journal.ppat.1007771.

33. Ko C, Chakraborty A, Chou WM, Hasreiter J, Wettengel JM, Stadler D, Bester R, Asen T, Zhang K, Wisskirchen K, McKeating JA, Ryu WS, Protzer U. 2018. Hepatitis B virus genome recycling and de novo secondary infection events maintain stable cccDNA levels. J Hepatol 69:1231–1241. https://doi.org/10.1016/j.jhep.2018.08.012.
34. Dezhbord M, Lee S, Kim W, Seong BL, Ryu WS. 2019. Characterization of the molecular events of covalently closed circular DNA synthesis in de novo hepatitis B virus infection of human hepatoma cells. Antiviral Res 163:11–18. https://doi.org/10.1016/j.antiviral.2019.01.004.
35. Qi Y, Gao Z, Xu G, Peng B, Liu C, Yan H, Yao Q, Sun G, Liu Y, Tang D, Song Z, He W, Sun Y, Guo JT, Li W. 2016. DNA polymerase kappa is a key cellular factor for the formation of covalently closed circular DNA of hepatitis B virus. PLoS Pathog 12:e1005893. https://doi.org/10.1371/journal.ppat.1005893.
36. Tu T, Zehnder B, Qu B, Urban S. 2021. De novo synthesis of hepatitis B virus nucleocapsids is dispensable for the maintenance and transcriptional regulation of cccDNA. JHEP Rep 3:100195. https://doi.org/10.1016/j.jhepr.2020.100195.
37. Jeong JK, Yoon GS, Ryu WS. 2000. Evidence that the 5'-end cap structure is essential for encapsidation of hepatitis B virus pregenomic RNA. J Virol 74:5502–5508. https://doi.org/10.1128/jvi.74.12.5502-5508.2000.
38. Ogilvie VC, Wilson BJ, Nicol SM, Morrice NA, Saunders LR, Barber GN, Fuller-Pace FV. 2003. The highly related DEAD box RNA helicases p68 and p72 exist as heterodimers in cells. Nucleic Acids Res 31:1470–1480. https://doi.org/10.1093/nar/gkg236.
39. Samaan S, Tranchevent LC, Dardenne E, Polay Espinoza M, Zonta E, Germann S, Gratadou L, Dutertre M, Auboeuf D. 2014. The Ddx5 and Ddx17 RNA helicases are cornerstones in the complex regulatory array of steroid hormone-signaling pathways. Nucleic Acids Res 42:2197–2207. https://doi.org/10.1093/nar/gkt1216.
40. Zhang H, Xing Z, Mani SK, Bancel B, Durantel D, Zoulim F, Tran EJ, Merle P, Andrisani O. 2016. RNA helicase DEAD box protein 5 regulates polycomb repressive complex 2/Hox transcript antisense intergenic RNA function in hepatitis B virus infection and hepatocarcinogenesis. Hepatology 64:1033–1048. https://doi.org/10.1002/hep.28698.
41. Liu Y, Nie H, Mao R, Mitra B, Cai D, Yan R, Guo JT, Block TM, Mechti N, Guo H. 2017. Interferon-inducible ribonuclease ISG20 inhibits hepatitis B virus replication through directly binding to the epsilon stem-loop structure of viral RNA. PLoS Pathog 13:e1006296. https://doi.org/10.1371/journal.ppat.1006296.
42. Yao Y, Yang B, Chen Y, Wang H, Hu X, Zhou Y, Gao X, Lu M, Niu J, Wen Z, Wu C, Chen X. 2019. RNA-binding motif protein 24 (RBM24) is involved in pregenomic RNA packaging by mediating interaction between hepatitis B virus polymerase and the epsilon element. J Virol 93:e02161-18. https://doi.org/10.1128/JVI.02161-18.
43. Sato S, Li K, Kameyama T, Hayashi T, Ishida Y, Murakami S, Watanabe T, Iijima S, Sakurai Y, Watashi K, Tsutsumi S, Sato Y, Akita H, Wakita T, Rice CM, Harashima H, Kohara M, Tanaka Y, Takaoka A. 2015. The RNA sensor RIG-I dually functions as an innate sensor and direct antiviral factor for hepatitis B virus. Immunity 42:123–132. https://doi.org/10.1016/j.immuni.2014.12.016.
44. Guo H, Jiang D, Zhou T, Cuconati A, Block TM, Guo JT. 2007. Characterization of the intracellular deproteinized relaxed circular DNA of hepatitis B virus: an intermediate of covalently closed circular DNA formation. J Virol 81:12472–12484. https://doi.org/10.1128/JVI.01123-07.
45. Yan R, Zhang Y, Cai D, Liu Y, Cuconati A, Guo H. 2015. Spinoculation enhances HBV infection in NTCP-reconstituted hepatocytes. PLoS One 10:e0129889. https://doi.org/10.1371/journal.pone.0129889.
46. Mao R, Zhang J, Jiang D, Cai D, Levy JM, Cuconati A, Block TM, Guo JT, Guo H. 2011. Indoleamine 2,3-dioxygenase mediates the antiviral effect of gamma interferon against hepatitis B virus in human hepatocyte-derived cells. J Virol 85:1048–1057. https://doi.org/10.1128/JVI.01998-10.
47. Kim S, Lee J, Ryu WS. 2009. Four conserved cysteine residues of the hepatitis B virus polymerase are critical for RNA pregenome encapsidation. J Virol 83:8032–8040. https://doi.org/10.1128/JVI.00332-09.
48. Dardenne E, Pierredon S, Driouch K, Gratadou L, Lacroix-Triki M, Espinoza MP, Zonta E, Germann S, Mortada H, Villemin JP, Dutertre M, Lidereau R, Vagner S, Auboeuf D. 2012. Splicing switch of an epigenetic regulator by RNA helicases promotes tumor-cell invasiveness. Nat Struct Mol Biol 19:1139–1146. https://doi.org/10.1038/nsmb.2390.
49. Kerns JA, Emerman M, Malik HS. 2008. Positive selection and increased antiviral activity associated with the PARP-containing isoform of human zinc-finger antiviral protein. PLoS Genet 4:e21. https://doi.org/10.1371/journal.pgen.0040021.
50. Cai D, Nie H, Yan R, Guo JT, Block TM, Guo H. 2013. A southern blot assay for detection of hepatitis B virus covalently closed circular DNA from cell cultures. Methods Mol Biol 1030:151–161. https://doi.org/10.1007/978-1-62703-484-5_13.
51. Guo H, Mao R, Block TM, Guo JT. 2010. Production and function of the cytoplasmic deproteinized relaxed circular DNA of hepadnaviruses. J Virol 84:387–396. https://doi.org/10.1128/JVI.01921-09.